

MSfusion: A Dynamic Model Splitting Approach for Resource-Constrained Machines to Collaboratively Train Larger Models

Jin Xie, Songze Li

Abstract—Training large models requires a large amount of data, as well as abundant computation resources. While collaborative learning (e.g., federated learning) provides a promising paradigm to harness collective data from many participants, training large models remains a major challenge for participants with limited resources like mobile devices. We introduce **MSfusion**, an effective and efficient collaborative learning framework, tailored for training larger models on resource-constrained machines through *model splitting*. Specifically, a double shifting model splitting scheme is designed such that in each training round, each participant is assigned a subset of model parameters to train over local data, and aggregates with sub-models of other peers on common parameters. While model splitting significantly reduces the computation and communication costs of individual participants, additional novel designs on adaptive model overlapping and contrastive loss functions help **MSfusion** to maintain training effectiveness, against model shift across participants. Extensive experiments on image and NLP tasks illustrate significant advantages of **MSfusion** in performance and efficiency for training large models, and its strong scalability: computation cost of each participant reduces significantly as the number of participants increases.

Index Terms—Collaborative Learning, Resource-constrained Devices, Double Shifting Model Splitting, Scalability.

I. INTRODUCTION

The contemporary technological landscape, characterized by the emergence and rapid evolution of large models, has ushered in a transformative era for machine learning and artificial intelligence. [1]–[5] Large language models (LLMs), exemplified by GPT and its counterparts, trained on vast corpora of billions of tokens, have captivated the global community with their remarkable capabilities, including human-like text generation, language translation, question answering, etc [6]–[10]. However, the practical training of these models is hamstrung by substantial computational and data requirements.

Consider the following real-world scenario: multiple companies, each armed with its own resource-limited servers (or cloud instances) and the private data collected from their respective clients, aspire to harness the advantages of large foundation models. The objective, therefore, is to leverage the existing computational power of their servers collaboratively to train a high-performance large model. Additionally, due to privacy and cost considerations, the introduction of an

additional central server is unsuitable for these companies. Conventional distributed learning methods like FedAVG [11] is not applicable as it is not practical to perform local SGD on large models, given the memory and computation constraints on companies’ local servers.

As demonstrated in [12], utilizing only 10% of a large language model during training can result in up to a 100-fold reduction in Floating Point Operations (FLOPs), translating to substantial cost savings. Motivated by this, we ask the following question: *Is it possible for these companies to collaboratively train a high-performance large model over their private data, with each company only training a sub-model as a split from the full model?*

To address the above question, we propose **MSfusion**, a novel collaborative learning framework that utilizes model splitting to enable effective and efficient training of larger models over resource constrained participants. **MSfusion** leverages a network of decentralized participants, each equipped with its own dataset, to independently extract and train split models from a larger model, effectively managing resource constraints. A novel double shifting splitting scheme is proposed to ensure extensive coverage of the global full model by the participants. An overlap aggregation method is introduced to further reduce communication needs. Moreover, an adaptive splitting mechanism is introduced to dynamically adjust the overlap of model parameters across participants as training progresses, expediting model convergence. A contrastive objective is designed to mitigate model drift caused by heterogeneous data distributions and differences in participants’ sub-models.

MSfusion, as a combination of model and data parallelism, not only reduces computation and communication costs, but also enhances the model performance via utilizing diverse datasets across multiple participants. We implement **MSfusion** and evaluate it over various image and NLP datasets. Extensive experiments demonstrate the substantial advantages of **MSfusion** in model performance and computation and communication efficiencies, over SOTA distributed learning methods using model splitting. **MSfusion** also exhibits strong scalability such that to achieve some target accuracy, the required split model size (hence computation/communication load) of each participant decreases significantly as the number participants increases. We view this as a key enabler for more resource-constrained participant to contribute to and benefit from training of large models.

Jin Xie is with the Internet of Things Thrust, The Hong Kong University of Science and Technology (Guangzhou), Guangzhou, China (email: jxie171@connect.hkust-gz.edu.cn).

Songze Li is with the School of Cyber Science and Engineering, Southeast University, Nanjing, China (e-mail: songzeli@seu.edu.cn).

II. RELATED WORKS

A. Decentralized Learning

Decentralized learning, in contrast to its centralized counterpart, pursues a consensus model through peer-to-peer communication, eliminating the reliance on a central server. [13]–[16] Commonly used decentralized FL like D-PSGD [17] offers distinct advantages in terms of communication efficiency and data privacy preservation when compared to Centralized Federated Learning (CFL). In an exemplary serverless, peer-to-peer FL implementation, [18] introduced BrainTorrent, which has found application in dynamic peer-to-peer FL environments, particularly in medical contexts. Dis-PFL is proposed in [19], which employs personalized sparse masks to train personalized models, reducing communication costs by filtering out parameter weights with minimal influence on the gradient.

B. KD-based Method

In the context of minimizing computation costs for participants, Knowledge Distillation (KD) emerges as a viable option. KD methods involve the server distilling intricate knowledge from a large model into a smaller, more manageable model, enabling clients to locally train on this distilled model. [20]–[23] Methods such as FedET in [24] have demonstrated some efficiency of KD. The defining strength of KD-based methods lies in their ability to train more compact models, approximating the performance of their larger counterparts with substantially less computational overhead. Nonetheless, achieving competitive accuracy typically necessitates access to public datasets that align in domain and scope with the client data [25]. However, a critical constraint of KD-based methods is the necessity for a central server, rendering them less suited to the decentralized collaborative settings introduced in this study.

C. Partial Model Training

The partial model training (PT-based) paradigm presents a distributive strategy wherein the model is fragmented across multiple servers, and each server is responsible for training a discrete segment of the model [26]–[28]. This modular approach considerably alleviates the computational demands on individual servers and fosters parallelized training. A notable limitation of current PT-based methodologies is their confinement to CFL frameworks, designed to reconcile computational disparities among clients. Such methods inherently assume that some participants possess the *complete* model during the training phase, a presumption misaligned with the decentralized scenario envisaged in our work. As we experimentally show later in Section V, without such participants, the performance of these methods degrades severely. [29] provide detailed analysis towards PT-based methods, further showing its potential for efficient collaborative training.

Distinction from split learning. We emphasize that the scenario considered in this work is drastically different from that of split learning [30]–[33], another collaborative training paradigm that splits model parameters between a powerful central server and one or multiple clients. In split learning,

the server and the clients work sequentially to train the entire model, through communicating intermediate data embeddings and gradients; a client cannot train its own sub-model independently due to missing gradients backpropagated from the server. While the key idea of split learning is to offload most of the computations on a powerful server, and requires the server and the clients to compute one after another, we focus on the scenario where all participants have similar computation capabilities, and each of them *independently* trains a smaller sub-model locally.

III. PROBLEM DEFINITION

Consider a collaborative learning system of N participants. Each participant n , $n \in [N] := \{1, \dots, N\}$, has a local dataset $\mathcal{D}_n = \{(x_i^{(n)}, y_i^{(n)})\}_{i=1}^{M_n}$ with M_n collected samples. The goal is to train a global model W over all participants' datasets, to solve the following optimization problem:

$$\begin{aligned} \min_W f(W) &= \frac{1}{N} \sum_{n=1}^N \hat{f}_n(W), \\ \text{s.t. } \hat{f}_n(W) &:= \frac{1}{M_n} \sum_{i=1}^{M_n} \hat{\mathcal{L}}(W; (x_i^{(n)}, y_i^{(n)})). \end{aligned} \quad (1)$$

Here $\hat{f}_n(W)$ is the local empirical risk of participant n , for some loss function $\hat{\mathcal{L}}$.

We focus on the scenarios of collaborative training of larger models on resource-constrained participants, where it is impractical for a participant to locally train W due to limited memory and computation resources. We consider a model splitting framework, such that each participant trains a smaller sub-model w_n split from the global full model W ($w_n \subseteq W$). Based on this, the local empirical risk for participant n becomes

$$f_n(w_n) := \frac{1}{M_n} \sum_{i=1}^{M_n} \mathcal{L}_n(w_n; (x_i^{(n)}, y_i^{(n)})), \quad (2)$$

where \mathcal{L}_n is the local loss corresponding to the sub-model w_n . After the participants finish their local training, the obtained sub-models are fused into a global model. This model fusion can take place over many rounds, and the sub-model trained at each participant can vary across rounds.

We define *split model size* of participant n , denoted by μ_n , as the ratio of the size of w_n to the size of W , i.e., $\mu_n = \frac{|w_n|}{|W|}$. In practice, μ_n is determined by the computation and communication capabilities of the participant. While previous studies have often assumed the presence of a powerful participant who can process the entire model, i.e., $\mu_n = 1$, we focus primarily on the scenarios where a group of resource-constrained participants collaborate to train an effective large model, where all participants have comparable but small split model sizes, e.g., $\mu_n \leq 0.5$ for all n .

Training large models over the collaborative learning framework described above are faced with following challenges.

- **Efficiency:** Computation cost for local training and communication cost to exchange models/gradients are major efficiency bottlenecks when dealing with large models

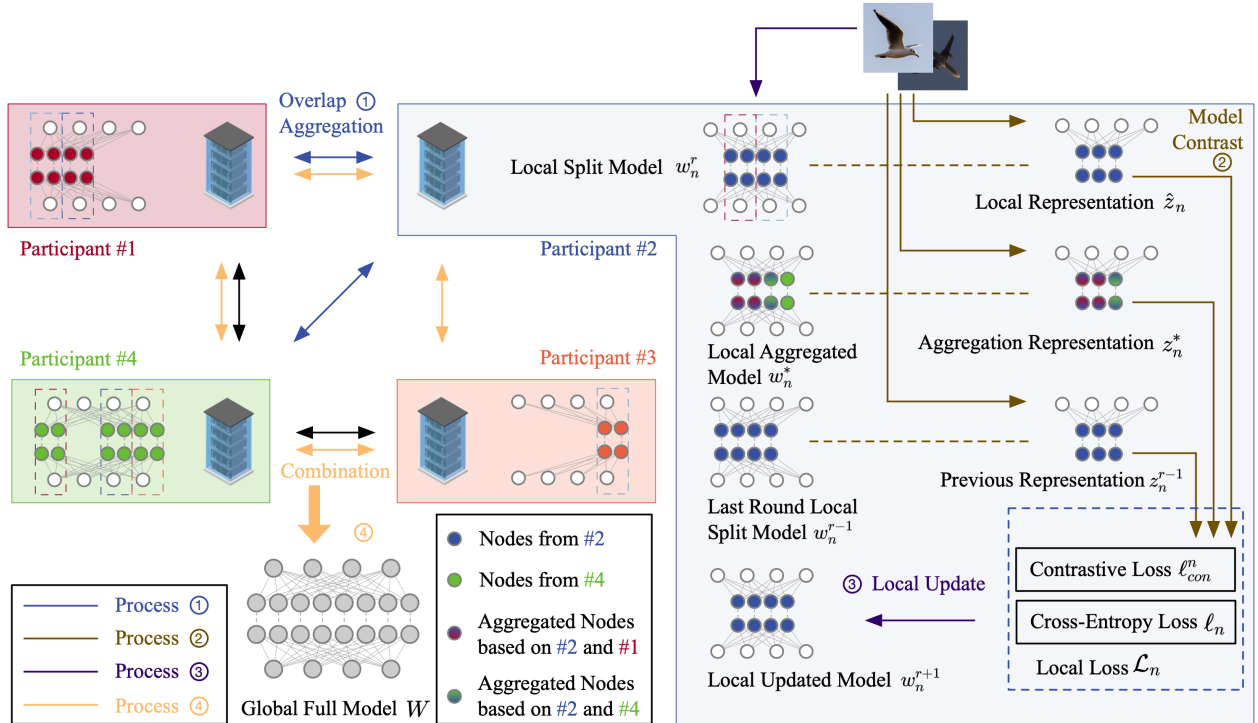


Fig. 1. Overview of MSfusion.

[34], [35]. Although model splitting helps to alleviate this issue, doing it naively may significantly reduce the model performance.

- **Data and model heterogeneity:** Like in FL, the local data on different participants tend to follow different distributions; in addition, the split portions of the global full model may diverge among participants. As it is well known that data non-iidness leads to reduced model performance [36]–[38], the “model drift” caused by double heterogeneity of sub-model and local data poses serious challenges on training effective large models.
- **Scalability:** To encourage participation of more resource-limited devices, it is desirable that as the number of participants increases, a smaller split model size is required on each participant to achieve a target accuracy. However, more participants exacerbates the issue of model drift, potentially degrading the model performance. How to design model splitting to maintain model performance with reduced split model size is hence crucial to achieving scalable collaborative training.

IV. MSFUSION

In this section, we introduce MSfusion, a model splitting approach to address the above challenges, for effective and efficient collaborative training of large models. Figure 1 provides an overview of proposed MSfusion. Algorithm 1 gives the pseudo-code of MSfusion.

A. Double shifting splitting scheme

We first introduce a novel splitting approach, dubbed Double Shifting Model Splitting Scheme (DSS), as essential part of

our MSfusion framework for achieving model partitioning among participants. MSfusion employs a two-tier shifting model partitioning approach: one at the inter-participant level and another at the inter-round level. This departs significantly from existing methodologies such as Federated Dropout, which utilizes random splitting; HeteroFL and FjORD, which employ static splitting; and FedRolex, which implements round-rolling splitting. Figure 2 shows the difference between DSS and previous model splitting schemes.

Inter-participant gap: During either the initiation phase of training or when there is a change in the set of participants (either through joining or leaving), each participant is assigned an unique index. For participants with adjacent indices, the starting nodes of their sub-models at i -th hidden layer of the global full model differs by the following gap

$$G_i = \frac{K_i}{N} \times c, \quad (3)$$

where K_i represents the size of i -th hidden layer, and $c \in [0, 1]$ serves as an overlapping control parameter. Consequently, the index of the starting node at participant n is nG_i . This gap ensures that the entirety of the global model W is adequately represented across all participants during a single communication round. Moreover, it ensures overlap (shade part in Figure 2) between sub-models assigned to adjacent participants.

Inter-round gap: Between successive communication rounds, each participant shifts the starting node of its local sub-model by a gap ζ . This gap ensures that the parameters of the global model W are uniformly optimized by individual participants.

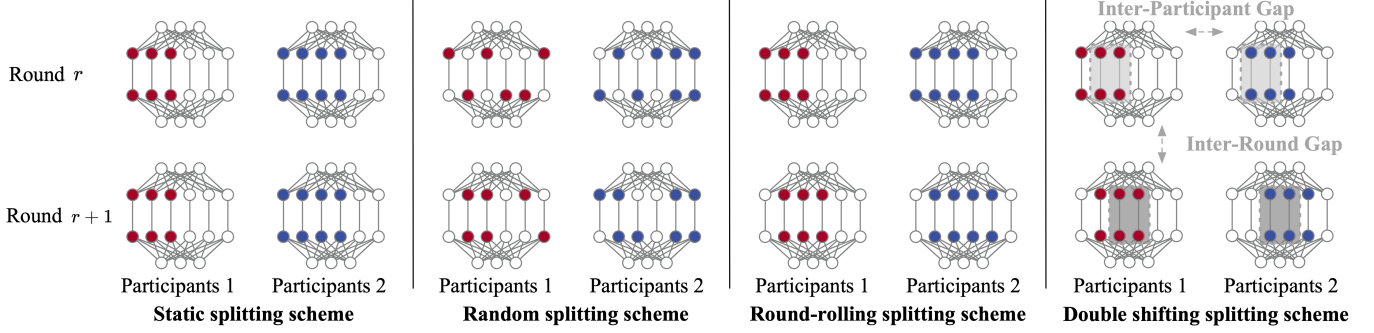


Fig. 2. Difference between DSS and previous model splitting schemes.

For a participant with index n and a split model size μ_n , for the i -th hidden layer of the global full model, the indices of the neurons (for fully-connected layers and hidden layers of attention heads of transformers) or filters (for convolutional layers) contained in the sub-model w_n in round r , denoted by $\varphi_{n,i}^{(r)}$, are presented as follows.

$$\varphi_{n,i}^{(r)} = \begin{cases} \{\mathcal{G}_{n,i,r}, \mathcal{G}_{n,i,r} + 1, \dots, \mathcal{G}_{n,i,r} + \lfloor \mu_n K_i \rfloor - 1\}, & \text{if } \mathcal{G}_{n,i,r} + \lfloor \mu_n K_i \rfloor \leq K_i, \\ \{\mathcal{G}_{n,i,r}, \mathcal{G}_{n,i,r} + 1, \dots, K_i - 1\} \cup & \\ \{0, 1, \dots, \mathcal{G}_{n,i,r} + \lfloor \mu_n K_i \rfloor - 1 - K_i\}, & \text{else.} \end{cases} \quad (4)$$

Here $\mathcal{G}_{n,i,r} = nG_{n,i} + r\zeta$ is the combined Inter-Participant and Inter-Round Gap. Note that in DSS the split model size μ dictates the number of output channels/neurons for the corresponding layer, which subsequently influences the number of input channels/neurons for the succeeding layer. To preserve dimensional consistency, DSS is intentionally not applied to the input and final output layers of the model.

B. Overlap aggregation

The introduction of DSS allows flexible designs for overlapped parameters between participants and across rounds. Specifically, the overlap rate (i.e., the ratio between the number of overlapped parameters and the total number of parameters in the full model) can be precisely quantified as $\delta_{\{n,n+1\}} = 1 - \frac{c}{\mu N}$ (with $c < \mu N$) for two adjacent participants with the same μ . For any pair of participants, their overlap rate δ is constrained within the range $[0, 1 - \frac{c}{\mu N}]$.

In each round r , MSfusion starts with exchanging overlapped model parameters among connected participants. That is, each participant n performs the following overlap aggregation:

$$\theta_{n,[l,i]}^* = \frac{1}{|S|+1} \sum_{s_i \in S} (\theta_{s_i,[l,i]}^r + \theta_{n,[l,i]}^r), \quad (5)$$

where $\theta_{n,[l,i]}^r$ donates the i -th parameter of layer l at participant n from w_n^r , $S \subset [N]$ is the set of connected participants holding $\theta_{n,[l,i]}^r$. This tailored aggregation around overlaps considerably reduces communication overhead from aggregation on full model size, enhancing the efficiency of distributed training of large models.

After overlap aggregation, each participant performs local training of its assigned sub-model on private data.

Algorithm 1 MSfusion

Input: Multi-participants set N_n , model split rate μ_n , local dataset \mathcal{D}_n , initial global full model W^0 , final stage parameter p .

Output: Participants maintained split model w_n^* , trained the global full model W^* .

Initiation: Assign an index to each participant based on network topology by consensus.

Per-Participant Operations:

for round $r < R$ **do**

if $r \bmod Q = 0$ **then**

 Update $c = c_0(1 - (r/R)p)$ in $\mathcal{G}_{n,i,r}$;

end if

 Split local w_n^r from W^r by DSS (4) with $\mathcal{G}_{n,i,r}$;

 Transmit $\theta_{n,[l,i]}^r$ to all connected participants holding i -th parameter;

 Receive $\theta_{s_i,[l,i]}^r$ from S connected participants holding i -th parameter;

 Aggregate local parameters based on (5);

 Update w_n^* based on $\theta_{n,[l,i]}^*$ and representations $z \leftarrow w_n^r$, $z^* \leftarrow w_n^*$, $z^{r-1} \leftarrow w_n^{r-1}$.

 Sample batch $b = \{(x_i, y_i)\}_{i=1}^B$ from \mathcal{D}_n ;

 The combined loss: $\mathcal{L}_n = \ell_n + \lambda \ell_{con}^n$, the contrastive loss (28);

 Update: $w_n^{r+1} \leftarrow w_n^r - \eta \nabla \mathcal{L}_n$;

 Receive round gap model parameter $\theta_{s,[l,i]}^{r+1}$ from connected participant.

end for

Global model combination:

 Transmit $\theta_{n,[l,i]}^R \in w_n^R$ to connected participants lacking i -th parameter;

 Receive $\theta_{s,[l,j]}^R \in \mathcal{C}_W w_n^R$ from connected participants holding j -th parameter;

 Combine $\theta_{n,[l,i]}^R$ with $\theta_{s,[l,j]}^R$ to obtain the global combined model W^* .

Dynamic overlap to boost convergence. As an optimization to speed up convergence, we further design a dynamic overlap strategy that periodically adjusts the overlapping control parameter c . For some adjustment period Q , MSfusion updates the parameter c in every Q rounds ($r \bmod Q = 0$) as

$$c = c_0(1 - (r/R)p), \quad (6)$$

where c_0 is the initial control parameter, p determines the final overlap rate, and R is the total round number.

As training progresses, c is tapered to amplify the overlap rate δ , such that updating each parameter utilizes data from more participants. The main idea behind this dynamic overlap strategy is that to cover as many as global model's parameters in the early stages of the training to obtain some basic model functionalities, and then focuses on addressing the model shift problem via fine-tuning each parameter with more participants' data.

C. Mathematical reasoning

In this section, we will provided a convergence analysis of a preliminary version of `MSfusion` with DSS and overlap aggregation for cross-entropy loss.

For the collaborative learning problem considered in the (1) with N participants and each with its own dataset $\mathcal{D}_n = \{(x_i^{(n)}, y_i^{(n)})\}_{i=1}^{M_n} \in \mathbb{R}^d \times \mathbb{R}$. It can be summarized as the following problem:

$$\begin{aligned} \min_W f(W) &= \frac{1}{N} \sum_{n=1}^N f_n(w_n), \\ \text{s.t. } f_n(w_n) &:= \frac{1}{K} \sum_{i=1}^K \mathcal{L}_n(w_n; (x_i, y_i)), \\ w_n &\subseteq W. \end{aligned} \quad (7)$$

In order to better investigate the DSS scheme, the definition of unbiased compressor is introduced following [29], [39].

Definition 1. Let $\zeta \geq 1$ and $\forall x \in \mathbb{R}^d$, for a (possibly random) mapping $\mathcal{C} : \mathbb{R}^d \rightarrow \mathbb{R}^d$, we say \mathcal{C} is unbiased compressor operators ($\mathcal{C} \in \mathbb{U}(\zeta)$) if the following holds:

$$\mathbb{E}[\mathcal{C}(x)] = x, \quad \mathbb{E}[\|\mathcal{C}(x)\|^2] \leq \zeta \|x\|^2. \quad (8)$$

Like for a random splitting scheme splitting $q \in [d] := \{1, \dots, d\}$ splitting the full model W , it can be viewed as a operator achieving the following

$$\mathcal{C}_{\text{Random}}(W) := \mathbf{C}_{\text{Rand}} W = \frac{d}{q} \sum_{i \in Q} e_i e_i^\top W, \quad (9)$$

where in random splitting scheme $Q \subseteq [d]$ is q random sampling (a subset of $[d]$ of cardinality q random chosen uniformly), e_1, \dots, e_d are standard unit basis vectors, and $\mathcal{C}_{\text{Random}}(W)$ belongs to $\mathbb{U}(\frac{d}{q})$, for a smaller size of split model (lower q), the higher the variance ζ of the compressor.

The Stochastic Gradient Descent (SGD) for participant n with local model w_n^r in round r can be written as:

$$w_n^{r+1} := w_n^r - \eta \nabla \mathcal{L}_n(w_n^r), \quad (10)$$

where η is the step size. In this paper, we consider the splitting scheme offers a sketch compressor $\mathbf{C}_n^r \in \mathbb{R}^d \times \mathbb{R}$ to achieve sketching on global full model W . And the split submodel computation can be represented as the following:

$$W^{r+1} = \mathbf{C}_n^r W^r - \eta \mathbf{C}_n^r \nabla \mathcal{L}_n(\mathbf{C}_n^r W^r). \quad (11)$$

The sketch \mathbf{C}_n^r requires to be symmetric positive semi-definite matrix. The ideal of (11) is to reduce the cost of directly

computation on full model W^r since the compressor \mathbf{C}_n^r ensure the update lies in a lower dimensional subspace. Each participant only compute its own the split model $w_n^r = \mathbf{C}_n^r W^r$, and we need this split model can effectively representing the global full model.

We mainly discuss the case where the global full model size is smaller than split model times participants number ($1 \leq \mu N$). In this situation, the Inter-Participant gap in DSS scheme ensures that the global full model W can be fully covered by participants in each round. That is in round r , we have inter-participant compressor

$$\mathbf{C}_{\text{part}}^r := \frac{1}{n} \sum_{i=1}^n \mathbf{C}_i^r = \mathbf{I}, \quad (12)$$

where \mathbf{I} is the identity matrix. And this means that in each round viewed from all the participants, the (11) is equivalent to the (10).

For the inter-round gap in DSS scheme ensures that the parameters of the global model W are uniformly optimized by individual participants. That is for participant n , there exist r^* to let the inter-round compressor

$$\mathbf{C}_{\text{round}}^n := \frac{1}{q^*} \sum_{i=1}^{r^*} \mathbf{C}_n^i = \mathbf{I}, \quad (13)$$

where $q^* \in [d]$ is determined by the split model rate μ . And this means means that for each participants viewed from finite round r^* , the (11) is equivalent to the (10).

Since from the Definition. 1, $\mathbb{E}[\|\mathcal{C}(x)\|^2] \leq \zeta \|x\|^2$, the overlapping parts can be viewed as an other unbiased overlapping compressor $\mathbf{C}_{\text{over}}^n$:

$$\mathbf{C}_{\text{over}}^n := N \cdot \sum_{j \in S} e_{\pi_j} e_{\pi_j}^\top, \quad (14)$$

where π_j is subset of $[d]$ determined by the overlapping part between participant j and participant n , and in `MSfusion` this can be controlled by c in dy_c . $S \subseteq N$ is a set of participants connected with n and have overlapping part.

Then we will make some commonly used assumptions to facilitate the analysis.

Assumption 2. The local loss function \mathcal{L}_n is \mathbf{L} -smooth (matrix smoothness [40], [41]) and u strongly convex. That is $\forall x, y \in \mathbb{R}^d$, there exist a positive semi-definite matrix $\mathbf{L} \succeq 0$

$$\mathcal{L}_n(y) \leq \mathcal{L}_n(x) + \langle \nabla \mathcal{L}_n(x), y - x \rangle + \frac{1}{2} \langle \mathbf{L}(y - x), y - x \rangle, \quad (15)$$

and for some $u > 0$

$$\mathcal{L}_n(y) \geq \mathcal{L}_n(x) + \langle \nabla \mathcal{L}_n(x), y - x \rangle + \frac{u}{2} \|y - x\|_2^2. \quad (16)$$

The standard (scalar) smoothness (L -smoothness) can be viewed as a special case of (15) with $\mathbf{L} = L \cdot \mathbf{I}$.

Assumption 3. In each communication round r , all the participant can computes the true gradient $\mathbf{C}_n^r \nabla \mathcal{L}_n(\mathbf{C}_n^r W^r)$ through its local submodel $w_n^r = \mathbf{C}_n^r W^r$.

To better study properties for DSS, we simplify the problem (7) into a quadratic problem

$$f(W) = \frac{1}{N} \sum_{n=1}^N f_i(w_n), \quad f_n(w_n) = \frac{1}{2} w_n^\top \mathbf{L}_n w_n - w_n^\top b_i. \quad (17)$$

And under this simplification, $f(x)$ is $\bar{\mathbf{L}}$ -smooth, and $\nabla f = \bar{\mathbf{L}}x - \bar{b}$ with $\bar{\mathbf{L}} = \frac{1}{N} \sum_{n=1}^N \mathbf{L}_i$ and $\bar{b} = \frac{1}{N} \sum_{n=1}^N b_i$.

We mainly examine the case of $b_i \equiv 0$, in this situation, the overall updating can be written as:

$$\frac{1}{N} \sum_{n=1}^N \mathbf{C}_n^r \nabla f_i(\mathbf{C}_n^r w_n) = \frac{1}{N} \sum_{n=1}^N \mathbf{C}_n^r \mathbf{L}_i \mathbf{C}_n^r w_n = \bar{\mathbf{B}}^r w_n^r. \quad (18)$$

Proved in [29], we have the following theorem.

Theorem 4. [29] Consider a distributed learning setting with learning process shown in (18) for a quadratic problem (17) with $\bar{\mathbf{L}} \succ 0$ and $b_i \equiv 0$. Then for $\bar{\mathbf{A}} := \frac{1}{2} \mathbb{E}[\bar{\mathbf{L}}\bar{\mathbf{B}}^r + \bar{\mathbf{L}}^r \bar{\mathbf{B}}] \succ 0$, there exists a constant $\xi > 0$.

$$\mathbb{E}[\bar{\mathbf{B}}^r \bar{\mathbf{L}} \bar{\mathbf{B}}^r] \preceq \xi \bar{\mathbf{A}}, \quad (19)$$

and for a step size $\eta (0 < \eta < \frac{1}{\xi})$ the iterates satisfy the following:

$$\frac{1}{R} \sum_{r=0}^{R-1} \mathbb{E} \left[\|\nabla f(w_n^r)\|_{\bar{\mathbf{L}}^{-1} \bar{\mathbf{A}} \bar{\mathbf{L}}^{-1}}^2 \right] \leq \frac{2(f(w_n^0) - \mathbb{E}[f(w_n^R)])}{\eta R}, \quad (20)$$

and

$$\mathbb{E} \left[\|w_n^r - w_n^*\|_{\bar{\mathbf{L}}}^2 \right] \leq \left(1 - \eta \lambda_{\min} \left(\bar{\mathbf{L}}^{-\frac{1}{2}} \bar{\mathbf{A}} \bar{\mathbf{L}}^{-\frac{1}{2}} \right) \right)^k \|w_n^r - w_n^*\|_{\bar{\mathbf{L}}}^2, \quad (21)$$

where $\lambda_{\min}()$ denotes minimum eigenvalue, $w_n^* := \arg \min f(w_n)$.

By applying Theorem 4, inter-participant compressor where $\mathbf{C}_{\text{part}}^r = \mathbf{I}$, we have $\bar{\mathbf{B}}^r = \bar{\mathbf{L}}$, $\bar{\mathbf{B}}^r \bar{\mathbf{L}} \bar{\mathbf{B}}^r = \bar{\mathbf{L}}^3$ and $\bar{\mathbf{A}} = \bar{\mathbf{L}}^2 \succ 0$. So the (19) is satisfied for constant $\xi = \lambda_{\max}(\bar{\mathbf{L}})$. And with a step size $\eta = \frac{1}{\xi}$, from (20) we have

$$\frac{1}{R} \sum_{r=0}^{R-1} \|\nabla f(w_n^r)\|_{\bar{\mathbf{L}}}^2 \leq \frac{2\lambda_{\max}(\bar{\mathbf{L}})(f(w_n^0) - f(w_n^R))}{R}. \quad (22)$$

Which means with inter-participant compressor viewed from all the participants the problem will converge. And the analysis is the same for inter-round compressor.

Then is the analysis for overlapping compressor $\mathbf{C}_{\text{over}}^n$. For the case each participant with same split model size μ , we have $f_n(w_n^r) = \frac{1}{2} w_n^{r\top} \mathbf{L} w_n^r$ with $\mathbf{L} \equiv \mathbf{L}_n$. If we define a diagonal matrix $\mathbf{D} = \text{diag}(\mathbf{L})$. And then 17 can be changed into

$$\begin{aligned} f_n(\mathbf{D}^{-\frac{1}{2}} w_n^r) &= \frac{1}{2} (\mathbf{D}^{-\frac{1}{2}} w_n^r)^\top \mathbf{L} (\mathbf{D}^{-\frac{1}{2}} w_n^r) \\ &= \frac{1}{2} (w_n^r)^\top (\mathbf{D}^{-\frac{1}{2}} \mathbf{L} \mathbf{D}^{-\frac{1}{2}}) w_n^r = \frac{1}{2} (w_n^r)^\top \hat{\mathbf{L}} w_n^r, \end{aligned} \quad (23)$$

where $\hat{\mathbf{L}} \succ 0$ as $\mathbf{L} \succ 0$, and $\text{diag}(\hat{\mathbf{L}}) = \mathbf{I}$. Since for each participant the overlapping rate with other participant is the same. Here we mainly analysis the overlapping part between

each two neighbor participant with biggest overlapping rate, then for overlapping compressor at each round r we have $\mathbf{C}_n^r = N \cdot e_{\pi_n^r} e_{\pi_n^r}^\top$, where π_n^r is the overlapping part between n and its neighbor with biggest overlapping rate. So we have

$$\mathbb{E}[\bar{\mathbf{B}}^r] = \mathbb{E} \left[\frac{1}{N} \sum_{n=1}^N \mathbf{C}_n^r \hat{\mathbf{L}}_i \mathbf{C}_n^r \right] = N \cdot \text{diag}(\hat{\mathbf{L}}) = N\mathbf{I}. \quad (24)$$

Then the 19 can be transformed as

$$\xi \hat{\mathbf{A}} = \xi N\mathbf{I} \succeq N^2 \mathbf{I}, \quad (25)$$

which holds with $\xi \geq N$. And the 20 can be converted to

$$\begin{aligned} \|\nabla f(w_n^r)\|_{\bar{\mathbf{L}}^{-1} \hat{\mathbf{A}} \bar{\mathbf{L}}^{-1}}^2 &\geq \\ N \lambda_{\min}(\hat{\mathbf{L}}^{-1}) \|\nabla f(w_n^r)\|_{\bar{\mathbf{L}}}^2 &= N \lambda_{\max}(\hat{\mathbf{L}}) \|\nabla f(w_n^r)\|_{\bar{\mathbf{L}}}^2. \end{aligned} \quad (26)$$

So the convergence guarantee for the overlapping compressor is

$$\frac{1}{R} \sum_{r=0}^{R-1} \|\nabla f(w_n^r)\|_{\bar{\mathbf{L}}}^2 \leq \frac{2\lambda_{\max}(\hat{\mathbf{L}})(f(w_n^0) - \mathbb{E}[f(w_n^R)])}{R}. \quad (27)$$

D. Contrastive objective

In the considered collaborative learning scenario, data on different participants often have distinct distributions, leaning to model shift after local training. In addition, model splitting across participants further exacerbate this drift, potentially undermining model performance. Other than dynamically adjusting the model overlap, we propose to adopt contrastive learning techniques [42]–[44] to further mitigate the model drift problem. However a direct application of contrastive FL methods from systems like MOON [45] or CreamFL [46] is untenable, since it is computationally infeasible to run global-local model contrast at the scale of full model size.

In MSfusion, we apply contrastive learning on sub-models to curb the divergence between a participant's local model and the corresponding aggregated model. For any input x , MSfusion extracts its local representation \hat{z}_n from the current sub-model w_n^r , the aggregation representation z_n^* from the local aggregated model w_n^* , and the previous representation z_n^{r-1} from the sub-model of last round w_n^{r-1} . Note there exist a inter-round shift between sub-models in consecutive rounds, and we focus on representations on the common part between w_n^r and w_n^{r-1} . We construct the contrastive loss in MSfusion as follows:

$$\begin{aligned} \ell_{\text{con}}^n &= \\ -\log &\frac{\exp\{[(\hat{z}_n)^T \cdot z_n^*]/\tau\}}{\exp\{[(\hat{z}_n)^T \cdot z_n^*]/\tau\} + \exp\{[(\hat{z}_n)^T \cdot z_n^{r-1}]/\tau\}}, \end{aligned} \quad (28)$$

where τ is the temperature coefficient to control the penalties on hard negative pairs [47]. This loss metric is optimized to align the local sub-model's representation closely with that of the aggregated model, thereby curtailing model drift.

The overall objective for participant n is then given by:

$$\mathcal{L}_n = \ell(w_n^r; x, y) + \lambda \ell_{\text{con}}^n. \quad (29)$$

TABLE I
DETAILS ABOUT DATASETS AND EXPERIMENT CONFIGURATIONS.

	CIFAR100	TinyImageNet	PennTreebank	WikiText2	WikiText103	WikiText103 (1B model)
Data/Token size	50,000	100,000	929,500	2,088,600	103,227,000	103,227,000
Local data/token size (10 participants)	5,000	10,000	92,950	208,860	10,322,700	10,322,700
Local epoch	1	1	1	1	1	1
Batch size	10	40	100	100	300	300
Model applied	ResNet18	ResNet18	Transformer	Transformer	Transformer	Transformer
Hidden size	[64, 128, 256, 512]	[64, 128, 256, 512]	[512, 512, 512, 512]	[512, 512, 512, 512]	[1024, 1024, 1024, 1024]	[512, 512, 512, 512]
Embedding Size		N/A	256	256	1024	1792
Number of heads		N/A	8	8	16	8
Dropout		N/A	0.2	0.2	0.2	0.2
Sequence length		N/A	64	64	64	64
Parameter size of global full model	11.2M	11.3M	7.32M	19.3M	574.92M	1.021B

TABLE II

GLOBAL MODEL ACCURACY AND COMPUTATION COST COMPARISON. SINCE FED-ET, FEDHM AND DEPTHFL DOES NOT OFFER DIRECTLY IMPLEMENT FOR LANGUAGE MODELING TASKS, THEY ARE NOT COMPARED IN NLP TASKS. FLOPs DENOTES THE FLOATING OPERATIONS FOR EACH PARTICIPANT PER ROUND. SIZE DENOTES THE LOCAL SPLIT MODEL SIZE FOR EACH PARTICIPANT. EXPERIMENTS ARE PERFORMED ON 10 PARTICIPANTS.

Methods	CIFAR100				TinyImageNet			
	iid	non-iid	FLOPs	μ_n	iid	non-iid	FLOPs	μ_n
HeteroFL	19.49 \pm 0.9	12.11 \pm 0.7	35.76M	25%	11.08 \pm 0.6	14.54 \pm 0.4	1.75B	62.5%
FedRolex	42.33 \pm 0.8	36.61 \pm 1.0	35.76M	25%	37.05 \pm 1.1	20.63 \pm 0.8	1.75B	62.5%
DepthFL	41.72 \pm 0.9	36.52 \pm 1.0	167M	30%	34.21 \pm 1.2	22.15 \pm 0.8	1.47B	55%
Fed-ET	41.61 \pm 0.4	35.78 \pm 0.5	1.09B	N/A	29.61 \pm 0.4	19.78 \pm 0.6	6.12B	N/A
FedHM	47.45 \pm 1.2	40.72 \pm 1.1	145.3M	40%	43.05 \pm 1.2	21.58 \pm 0.6	1.43B	40%
MSfusion S	43.77 \pm 0.5	37.01 \pm 0.7	6.95M	10%	12.62 \pm 0.7	11.45 \pm 0.5	79.79M	12.5%
MSfusion M	50.04 \pm 0.5	44.11 \pm 0.4	22.33M	18.75%	39.61 \pm 0.6	20.91 \pm 0.6	297.0M	25%
MSfusion L	60.63 \pm 0.4	47.21 \pm 0.5	151.7M	50%	51.41 \pm 0.4	24.67 \pm 0.3	1.26B	50%

Methods	PennTreebank			WikiText2			WikiText103			WikiText103 (1B model)		
	Perplexity	Size	μ_n	Perplexity	Size	μ_n	Perplexity	Size	μ_n	Perplexity	Size	μ_n
HeteroFL	55.97 \pm 5.4	5.09M	75%	579.05 \pm 8.4	104.02M	75%	763.44 \pm 26	426.34M	75%	N/A	N/A	
FedRolex	61.52 \pm 6.8	5.09M	75%	547.32 \pm 45	104.02M	75%	653.76 \pm 35	426.34M	75%	N/A	N/A	
MSfusion S	9.09 \pm 0.7	1.24M	21.875%	44.33 \pm 3.6	30.33M	18.75%	21.45 \pm 2.8	121.49M	21.875%	6.34 \pm 0.4	213.11M	21.875%
MSfusion M	8.02 \pm 0.5	1.43M	25%	5.28 \pm 0.4	34.65M	25%	7.94 \pm 0.6	139.02M	25%	5.59 \pm 0.3	244.07M	25%
MSfusion L	3.11 \pm 0.2	3.13M	50%	3.59 \pm 0.2	69.23M	50%	5.24 \pm 0.3	281.04M	50%	5.03 \pm 0.3	495.63M	50%

Here ℓ is cross-entropy loss, and λ is the coefficient governing the weight of the contrastive loss.

After the training process, an efficient fusion mechanism within MSfusion fetches the requisite global model. Participants engage with adjacent peers to retrieve missing parameters (complementary set $\mathcal{C}_{K_i} \Theta_{n,i}^{(r)}$), and combine them with aggregated overlap parameters, obtaining the global full model W^* for further inference.

V. EXPERIMENTS

In this section, we present a comprehensive evaluation of MSfusion on various benchmark datasets, including both image classification and natural language processing (NLP) tasks.

Datasets. We conduct our evaluations on two distinct task categories: image classification and NLP. For image classification, our method is subjected to rigorous testing on two widely recognized datasets: CIFAR100 [48] and TinyImageNet [49]. For NLP tasks, we adopt the method in [27], [28], [50], dividing the data samples from the original dataset onto each participant uniformly at random. As a result, the number of possible words in each participant’s local dataset is approximately 1,000 for PennTreebank [51]; 3,000 for WikiText2; and 50,000 for WikiText103. However, all participants use the

same table for the tokenizer, with the full vocabulary of the entire dataset.

Models. To underscore the versatility of our approach across varied architectures, we employ both convolutional and transformer models in our experiments. In image classification tasks, a modified ResNet18 following [28] is employed. Additionally, we showcase the transformative potential of MSfusion by demonstrating its efficacy in handling LLMs. Specifically, transformer models are deployed for our NLP tasks. The global full model parameter sizes for adopted transformers are 7.32M for PennTreebank, 19.3M for WikiText2, 574.92M for WikiText103, and 1.021B for WikiText103.

Data heterogeneity. In the image classification tasks, we introduce data heterogeneity by deliberately skewing the label distribution among participants. This non-iid characteristic is attained by assigning each participant a distinct subset of H classes. Specifically, for CIFAR100, we set $H = 20$, and for TinyImageNet, $H = 40$. Moreover, for NLP tasks, we naturally generate non-IID data distribution through dataset partitioning among participants. As a result, the vocabulary size is reduced for each participants. Specifically, in WikiText2, the vocabulary size is reduced from a total of 33,728 words to approximately 3,000 words. In PennTreebank, the vocabulary is reduced from 10,000 to approximately 1,000 words, and in WikiText103, it is scaled down from 267,735

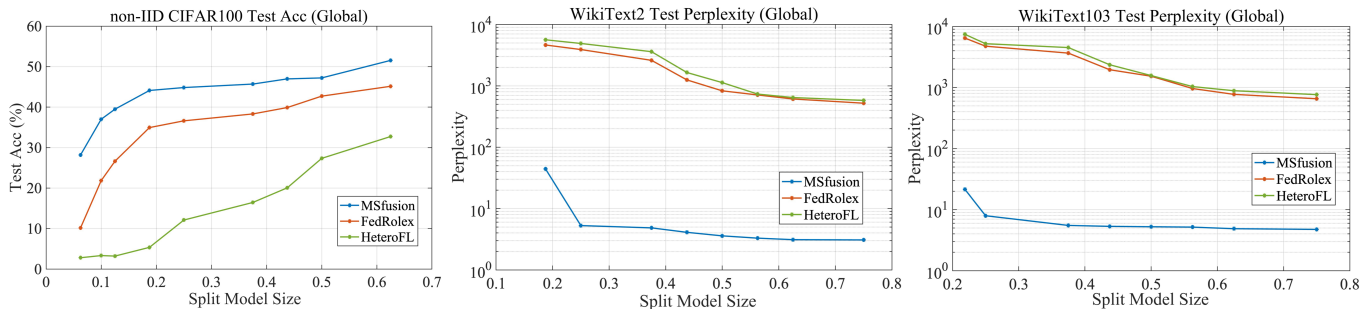


Fig. 3. Performance comparisons on non-IID CIFAR100, WikiText2 and WikiText103 datasets.

to approximately 50,000 words.

Model splitting. We focus on participants with *uniformly* small model splits $\mu_n \in \{6.25\%, 10\%, \dots, 62.5\%\}$. The global full model represents an unsplit, complete model. *There is no participant with $\mu_n = 1$.* This is a notable advantage compared to previous works with heterogeneous settings. While a participant training the full model plays an important role in maintaining model performance, it is not present in our case due to large model size and the focus on resource-constrained settings. To create local sub-models, we adjust the number of kernels in convolution layers of ResNet18 while keeping the output layer nodes constant. For Transformer models, we vary the number of nodes in the hidden layers of the attention heads. We set the inter-round gap for DSS $\zeta = 1$, the initial overlapping control parameter $c_0 = 1$, and the adjustment period $Q = 10$.

Baselines. We compare MSfusion against FedHM [52], DepthFL [50], SOTA PT-based model-heterogeneous FL methods including HeteroFL [28] and FedRolex [27], as well as SOTA KD-based FL method Fed-ET [24]. For FedHM, it leverages low-rank decomposition to reduce communication costs and training overhead. However, its reliance on server-side matrix decomposition introduces additional computational demands, particularly with large transformer models. For DepthFL, it adopts a strategy where clients train local models at depths commensurate with their resource capabilities, utilizing self-distillation to enhance the training of deeper layers. For experiments with a ring topology, we compare MSfusion with a widely used decentralized learning algorithm D-PSGD [17], and the SOTA decentralized personalized FL algorithm Dis-PFL [19] with sparse training technique.

Hyperparameters and Platform. For all the experiments, SGD optimizer is applied. The communication round for CIFAR100 experiments is 500, for TinyImageNet, PennTreebank and WikiText2 experiments is 800, for WikiText103 experiments is 100. Local epoch for participants is 1. $\tau = 0.5$ like in [42]. $\lambda = 1$ following [45]. The initial control parameter $c_0 = 0.4$, and final stage parameter $p = 0.75$. Table I present the parameter size, data partition, and model architecture for each experiment.

Learning rate scheduler for MSfusion is CyclicLR scheduler which varies the learning rate between the minimal and maximal thresholds. The learning rate values change in a cycle from more minor to higher and vice versa. The reasons for choosing CyclicLR is the dynamic mechanisms

in MSfusion. The minimal thresholds is set 0.001, the maximal is set 0.0012, the cycle round is the same with the maximum communication round. Note to ensure equitable comparisons, we maintain uniformity in parameters across all PT-based baselines (HeteroFL and FedRolex), including learning rate, and the number of communication rounds. Other hyperparameters of FedRolex and HeteroFL is set by following [27].

All experiments are conducted using PyTorch version 2.0 on a single machine equipped with two Intel platinum 8378A CPUs, 512GB of memory, and eight NVIDIA A6000 GPUs.

A. Performance

Performance and computational cost comparisons between MSfusion and the aforementioned baselines are summarized in Table II. Performance metrics are evaluated by testing the final global model on the testing dataset. For WikiText103 with 1B global full model, HeteroFL and FedRolex fail to converge. To ensure equitable comparisons with centralized methods, we apply fully connected topology for MSfusion in these experiments. For Fed-ET, we also include the computation cost of the server and average it across participants. For FedHM, the computation cost of matrix decomposition is calculated, where we set a fixed and uniform rank ratio γ for all clients. And for DepthFL, we set a uniform class depth of a for all clients in CIFAR100 and a uniform class depth of c for all clients in TinyImageNet.

Table II reveals that, particularly for CIFAR100 datasets, MSfusion S outperforms HeteroFL and FedRolex with only 10% of the full model per participant, with less than 20% of the computational cost. Increasing the local split model size directly enhances overall performance, though it comes at the cost of increased computation. MSfusion M achieves similar performance with Fed-ET and outperforms all other baselines, in the more complex TinyImageNet dataset. MSfusion L outperforms Fed-ET for both image datasets while taking only 20% of the computation. Additionally, it's important to note that MSfusion does not require a central server and does not rely on public data, in contrast to KD-based methods. In NLP tasks, MSfusion significantly outperforms HeteroFL and FedRolex. The suboptimal performance of HeteroFL and FedRolex in collaborative training larger models is due to massive untrained global model parameters per round and exacerbated model drift in transformer models,

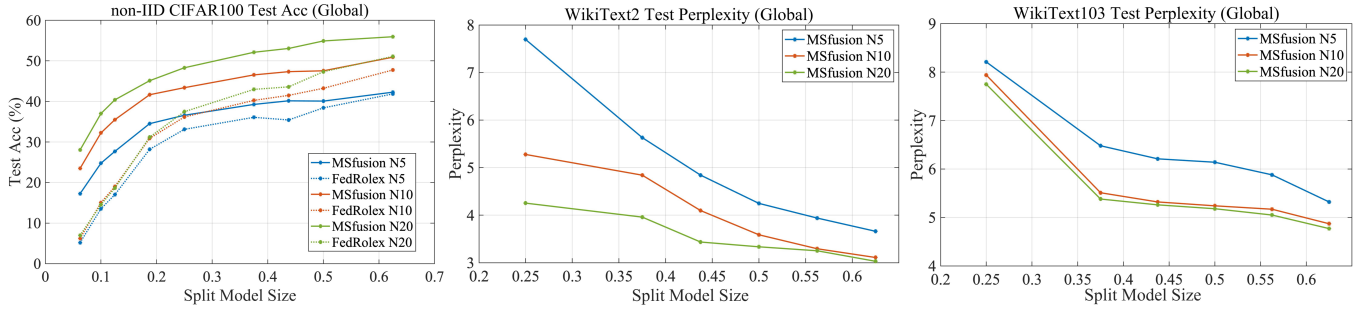


Fig. 4. Performance of MSfusion for different numbers of participants.

issues unaddressed in their splitting-focused methodologies. While these problems can be efficiently tackled by DSS and designed contrastive loss in MSfusion further emphasizes the advantage of MSfusion in handling larger models. It is also shown that while DepthFL and FedHM exhibit improved model accuracy over HeteroFL and FedRolex, MSfusion still obtains a better performance with less computation cost.

Performance comparisons with split model size for CIFAR100, WikiText2 and WikiText103 are shown in Figure 3. The performance advantage of MSfusion is substantial, especially for smaller split model sizes, due to the more effective DSS scheme. To achieve a target accuracy, much smaller split model size is required for MSfusion, resulting in significantly lower computation and communication costs at all participants. Like for CIFAR100, for a target 40% accuracy performance, FedRolex requires about 45% split model size which costs 116M FLOPs, while MSfusion only requires 12.5% split model size which only costs 9.83M FLOPs. That is, to train a global model with the same performance, a MSfusion participant incurs less than one tens of the computation cost of a FedRolex participant.

The results of an ablation study on CIFAR100 and WikiText2 with $\mu = 18.75\%$ is given in Table III. It shows the accuracy and computation comparison for MSfusion, MSfusion without contrastive objective (w/o Con), MSfusion without dynamic overlap (w/o Dyn), and MSfusion without both (w/o Con & Dyn). The results showcase MSfusion’s superior performance over all baselines. Specifically, the performance gain of MSfusion is more prominent for NLP tasks. This is mainly attributed to the relatively larger size of local model split within the transformer architecture, further amplifying the model drift problem. This study demonstrates that the proposed contrastive objective and dynamic overlap techniques play key roles in ensuring the effectiveness of MSfusion training, with a marginal increase in computational cost. Moreover, we note that MSfusion without contrastive objective still outperforms all PT-based methods with much less computation cost.

B. Scalability

To assess scalability of MSfusion, we conduct experiments on different numbers of participants, where each participant holds 5% of the training dataset. As shown in Figure 4, MSfusion consistently outperforms the SOTA FedRolex

TABLE III
PERFORMANCE AND COMPUTATIONAL COSTS OF BASELINES AND MSFUSION VARIANTS.

Methods	CIFAR100 ACC	FLOPs	WikiText2 PPL	FLOPs
HeteroFL	12.11 \pm 0.7	35.76M	579.05 \pm 8.4	1.08B
FedRolex	36.61 \pm 1.0	35.76M	547.32 \pm 4.5	1.08B
MSfusion w/o Con	40.96 \pm 0.4	20.32M	9.57 \pm 2.1	257.2M
MSfusion w/o Dyn	41.48 \pm 0.4	22.33M	7.35 \pm 1.5	290.1M
MSfusion w/o Con & Dyn	39.77 \pm 0.5	20.32M	11.24 \pm 2.3	257.2M
MSfusion	44.11 \pm 0.4	22.33M	5.276 \pm 0.4	290.1M

for all participant counts. Notably, for small split model sizes, introducing more participants does not help to improve the performance of FedRolex, as it does not properly address the issue of model drift. For MSfusion, the model performance improves at all split model sizes as the number of participants increases; to achieve a target level of performance, as participants increases, the required split model size on each participant reduces significantly. For instance for WikiText2, to achieve a target PPL around 4, the split model size reduces from 56.26% with 5 participants to merely 37.5% with 20 participants. This makes MSfusion a key enabler for resource-constrained machines to contribute to and benefit from collaborative training.

C. Topology

In scenarios with limited network resources, we may need to utilize a ring topology for participants to communicate. Figure 5(a) illustrates the distinction between the ring topology and the fully-connected topology. We examine the performance of MSfusion under these two network topologies, as detailed in Figure 5(b). We find that under the ring topology, MSfusion is able to achieve a sizable portion of the full performance achieved used fully-connected topology, and the gap is rather marginal for the most relevant split model sizes of 25% \sim 45%. Also, operating MSfusion under the ring topology still attains the desirable scalability with number of participants.

TABLE IV
ACCURACY, COMMUNICATION COST (COMM), AND COMPUTATION COST (FLOPs) COMPARISON OF CIFAR-100 FOR RING TOPOLOGY.

Methods	Local ACC	COMM	FLOPs
Dis-PFL	52.57 \pm 0.3	44.8MB	700.1M
D-PSGD	13.38 \pm 0.5	89.7MB	830.3M
MSfusion	56.57 \pm 0.6	2.85MB	22.33M

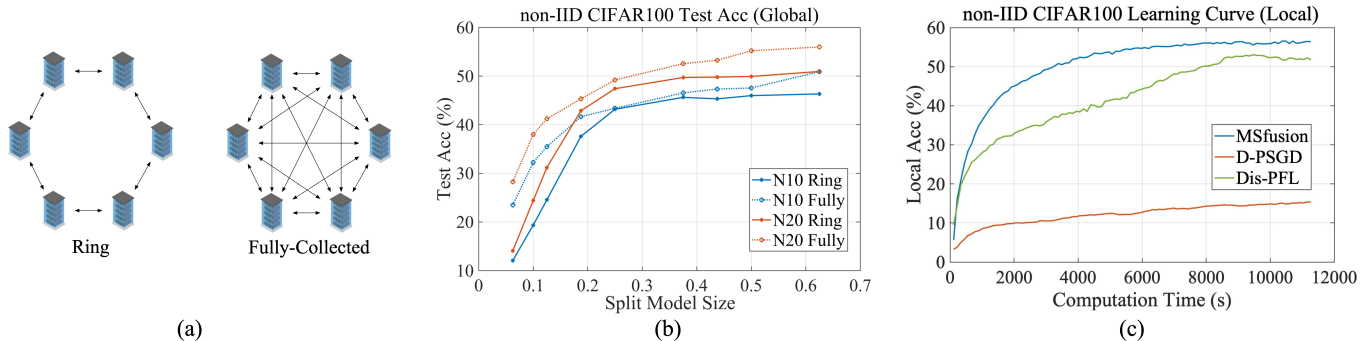


Fig. 5. (a) Illustrations of ring and fully-connected network topology; (b) Performance of MSfusion under ring and fully-connected topology; (c) Performance comparison under ring topology (MSfusion $\mu = 25\%$ for all participants).

Figure 5(c) shows the performance comparison between MSfusion, Dis-PFL, and D-PSGD. As in both Dis-PFL and D-PSGD, each participant retains a personalized model, and accuracy is calculated as the average of local accuracies, we measure the average accuracy of the global model trained using MSfusion on local datasets. We can see that MSfusion converges much faster and outperforms both baselines. Additionally, the model accuracy, and the average communication and computation costs for CIFAR-100 are compared in Table IV. MSfusion achieves better performance with less than 5% communication and computation costs, corroborating the effectiveness and efficiency of its overlap averaging mechanism.

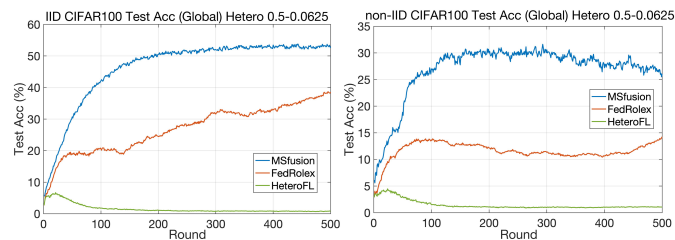


Fig. 6. Heterogeneous split model size comparison ($\mu_n \in \{0.5, 0.25, 0.1875, 0.125, 0.0625\}$)

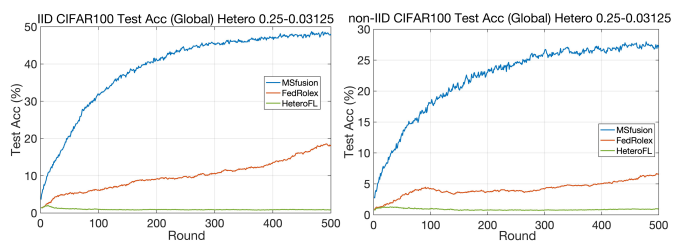


Fig. 7. Heterogeneous split model size comparison ($\mu_n \in \{0.25, 0.1875, 0.125, 0.0625, 0.03125\}$)

D. Heterogeneous split fusion setting

We also discuss the heterogeneous split fusion setting where participants' server with different computation power are collaboratively training a large model. Specifically, in this paper, our heterogeneous setting is more constrained with split model size for all participants is less than half of the global full model ($\forall \mu_n \leq 0.5$). Figure 6 shows the heterogeneous split model size comparison with

($\mu_n \in \{0.5, 0.25, 0.1875, 0.125, 0.0625\}$), Figure 7 shows the heterogeneous split model size comparison with ($\mu_n \in \{0.25, 0.1875, 0.125, 0.0625, 0.03125\}$). In these experiments, total of 10 participants are involved in the collaboratively training process, each 2 are assigned with a fixed unique split model size from the list sets. It is clear that the proposed MSfusion way outperformed STOA PT-based methods in the more constrained heterogeneous collaboratively learning settings in both IID and non-IID data distributions with much faster converge speed and higher accuracy. FedRolex and outperform HeteroFL with its round-rolling scheme, but the performance of FedRolex is greatly dropped with smaller split model size in Figure 7. While MSfusion can still maintain a good performance thanks to its much more efficient DSS scheme. It can also be observed that the model heterogeneous will greatly enhance the model drift between the participants resulting greatly influence the performance in the non-IID settings.

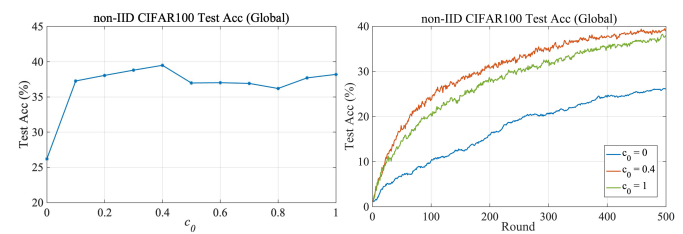


Fig. 8. Effect of initial overlapping control parameter c_0 .

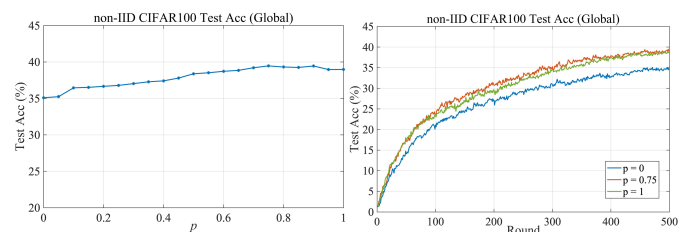


Fig. 9. Effect of overlapping final stage parameter p .

E. Ablation study

An ablation study toward the effect of initial overlapping control parameter c_0 is given in Figure 8. Specifically, it

TABLE V
MSFUSION PERFORMANCE OF FULL MODEL AND LOCAL SPLIT MODEL.

Method	non-iid CIFAR100			WikiText2		
	ACC	Split ACC	FLOPs	Perplexity	Split Perplexity	Size
MSfusion $\mu = 100\%$	52.61 \pm 0.7	52.61 \pm 0.7	572.2M	3.26 \pm 0.2	3.26 \pm 0.2	139.01M
MSfusion $\mu = 18.75\%$	44.11 \pm 0.4	39.54 \pm 0.4	22.33M	44.33 \pm 3.6	68.73 \pm 5.4	30.33M
MSfusion $\mu = 50\%$	47.21 \pm 0.5	41.28 \pm 0.6	151.7M	3.59 \pm 0.2	5.69 \pm 0.5	69.23M

demonstrates that a $c_0 = 1$ setting leads to slightly faster convergence than $c_0 = 0.4$ during the initial stages of training, both outperforming the $c = 0$ scenario where the global full model shows insufficient training initially. This evidence supports the insufficient convergence at the beginning of training. Furthermore, thanks to a larger overlap in parameters between local models and hence reduced model drift, $c_0 = 0.4$ starts to outperform $c_0 = 1$ after the initial stages of training.

We also provide ablation study on the effect of parameter p that controls the final overlap rate (i.e., the overlap rate $c = c_0(1 - \frac{r}{R}p)$ at round r), reflected in Figure 9. Specifically, we observed that a p value of 0, which implies a constant c , leads to performance degradation due to client drift. Conversely, increasing p narrows the inter-participant gap as the training progresses, enhancing the model’s ability to leverage data from a broader range of participants. However, excessively high p values can hinder convergence speed, as evidenced by the learning curve where $p = 0.75$ achieves faster convergence over $p = 1$. Thus, we identified $p = 0.75$ as the optimal parameter for a faster convergence to a higher accuracy.

TABLE VI
MSFUSION PERFORMANCE WITH DIFFERENCE SEQUENCE LENGTHS (SMALLER PERPLEXITY IS BETTER), SPLIT MODEL SIZE $\mu = 25\%$.

Sequence Length	PennTreebank	WikiText2	WikiText103
	Perplexity	Perplexity	Perplexity
64	8.02 \pm 0.5	5.28 \pm 0.4	7.94 \pm 0.6
256	8.41 \pm 0.4	5.75 \pm 0.4	8.14 \pm 0.6
512	10.11 \pm 0.6	6.31 \pm 0.5	9.47 \pm 0.7

F. Additional experiments

Performance of full model and local split model. We also evaluated the performance of model without splitting ($\mu = 100\%$) and the local split model performance on the global test dataset. Results are shown in Table V. The ACC and Perplexity is the performance of combined global full model, and Split ACC and Split Perplexity is the local split model performance averaged over all participants on the global test dataset.

We observe that MSfusion with $\mu = 50\%$ achieves a comparable performance with $\mu = 100\%$, with much less computation cost. This tradeoff is acceptable or even desirable in scenarios where the training is limited by the computation, storage and communication resources. Besides, for $\mu < 100\%$, there is a sizable performance loss on the local split model. This is due to 1) larger number of parameters in the full model; and 2) training over other participants’ datasets.

Different sequence length. We adopted a sequence length of 64 to make a fair comparison with prior works on federated learning with model splitting [27], [28], [50], which used a

sequence length of 64 in their experiments. Another reason to use a smaller sequence length is to reduce computation complexities, since this work focuses on resource-constrained participants. However, we also note that more commonly used sequence lengths should be considered, and we provided experiments on sequence lengths of 256 and 512. Results are reported in Table VI, it indicates that MSfusion maintains its effectiveness across a broader range of sequence lengths, achieving comparable performance as the sequence length increases. This result underscores the robustness of MSfusion in accommodating various NLP task requirements.

VI. CONCLUSION AND DISCUSSION

We introduce MSfusion to address the challenge in collaboratively training large models on resource-constrained machines. Through an ensemble of novel techniques like DSS, dynamic model split and aggregation, and contrastive loss design, MSfusion achieves superior performance with significantly reduced complexity. Our empirical results underscore the potential of MSfusion to collaboratively training large models for CV and NLP tasks, offering a promising solution for organizations striving to maximize performance while judiciously managing resources.

While the primary focus of MSfusion is on optimizing the performance of training larger models in a resource-constrained, decentralized environment, we also recognize the importance of privacy concerns, and have designed MSfusion to be readily compatible with well-established privacy-preserving mechanisms like Differential Privacy (DP) and Secure Aggregation [53], [54], further protecting participants’ data privacy.

REFERENCES

- [1] T. Brown, B. Mann, N. Ryder, M. Subbiah, J. D. Kaplan, P. Dhariwal, A. Neelakantan, P. Shyam, G. Sastry, A. Askell *et al.*, “Language models are few-shot learners,” *Advances in neural information processing systems*, vol. 33, pp. 1877–1901, 2020.
- [2] L. Floridi and M. Chiriatti, “Gpt-3: Its nature, scope, limits, and consequences,” *Minds and Machines*, vol. 30, pp. 681–694, 2020.
- [3] S. Zhang, S. Roller, N. Goyal, M. Artetxe, M. Chen, S. Chen, C. Dewan, M. Diab, X. Li, X. V. Lin *et al.*, “Opt: Open pre-trained transformer language models,” *arXiv preprint arXiv:2205.01068*, 2022.
- [4] A. Chowdhery, S. Narang, J. Devlin, M. Bosma, G. Mishra, A. Roberts, P. Barham, H. W. Chung, C. Sutton, S. Gehrmann *et al.*, “Palm: Scaling language modeling with pathways,” *Journal of Machine Learning Research*, vol. 24, no. 240, pp. 1–113, 2023.
- [5] J. Achiam, S. Adler, S. Agarwal, L. Ahmad, I. Akkaya, F. L. Aleman, D. Almeida, J. Altenschmidt, S. Altman, S. Anadkat *et al.*, “Gpt-4 technical report,” *arXiv preprint arXiv:2303.08774*, 2023.
- [6] A. Radford, K. Narasimhan, T. Salimans, I. Sutskever *et al.*, “Improving language understanding by generative pre-training,” 2018.
- [7] J. Devlin, M.-W. Chang, K. Lee, and K. Toutanova, “Bert: Pre-training of deep bidirectional transformers for language understanding,” *arXiv preprint arXiv:1810.04805*, 2018.

- [8] C. Raffel, N. Shazeer, A. Roberts, K. Lee, S. Narang, M. Matena, Y. Zhou, W. Li, and P. J. Liu, "Exploring the limits of transfer learning with a unified text-to-text transformer," *Journal of machine learning research*, vol. 21, no. 140, pp. 1–67, 2020.
- [9] R. Bommasani, D. A. Hudson, E. Adeli, R. Altman, S. Arora, S. von Arx, M. S. Bernstein, J. Bohg, A. Bosselut, E. Brunskill *et al.*, "On the opportunities and risks of foundation models," *arXiv preprint arXiv:2108.07258*, 2021.
- [10] W. X. Zhao, K. Zhou, J. Li, T. Tang, X. Wang, Y. Hou, Y. Min, B. Zhang, J. Zhang, Z. Dong *et al.*, "A survey of large language models," *arXiv preprint arXiv:2303.18223*, 2023.
- [11] B. McMahan, E. Moore, D. Ramage, S. Hampson, and B. A. y Arcas, "Communication-efficient learning of deep networks from decentralized data," in *Artificial intelligence and statistics*. PMLR, 2017, pp. 1273–1282.
- [12] N. Dey, G. Gosal, Zhiming, Chen, H. Khachane, W. Marshall, R. Pathria, M. Tom, and J. Hestness, "Cerebras-gpt: Open compute-optimal language models trained on the cerebras wafer-scale cluster," 2023.
- [13] L. Wang, Y. Xu, H. Xu, M. Chen, and L. Huang, "Accelerating decentralized federated learning in heterogeneous edge computing," *IEEE Transactions on Mobile Computing*, 2022.
- [14] L. Yuan, Z. Wang, L. Sun, S. Y. Philip, and C. G. Brinton, "Decentralized federated learning: A survey and perspective," *IEEE Internet of Things Journal*, 2024.
- [15] S. Chen, Y. Xu, H. Xu, Z. Ma, and Z. Wang, "Enhancing decentralized and personalized federated learning with topology construction," *IEEE Transactions on Mobile Computing*, no. 01, pp. 1–16, 2024.
- [16] T. Sun, D. Li, and B. Wang, "Decentralized federated averaging," *IEEE Transactions on Pattern Analysis and Machine Intelligence*, vol. 45, no. 4, pp. 4289–4301, 2022.
- [17] X. Lian, C. Zhang, H. Zhang, C.-J. Hsieh, W. Zhang, and J. Liu, "Can decentralized algorithms outperform centralized algorithms? a case study for decentralized parallel stochastic gradient descent," *Advances in neural information processing systems*, vol. 30, 2017.
- [18] A. G. Roy, S. Siddiqui, S. Pölsterl, N. Navab, and C. Wachinger, "Braitorrent: A peer-to-peer environment for decentralized federated learning," *arXiv preprint arXiv:1905.06731*, 2019.
- [19] R. Dai, L. Shen, F. He, X. Tian, and D. Tao, "Dispfl: Towards communication-efficient personalized federated learning via decentralized sparse training," *arXiv preprint arXiv:2206.00187*, 2022.
- [20] J. Gou, B. Yu, S. J. Maybank, and D. Tao, "Knowledge distillation: A survey," *International Journal of Computer Vision*, vol. 129, no. 6, pp. 1789–1819, 2021.
- [21] J. H. Cho and B. Hariharan, "On the efficacy of knowledge distillation," in *Proceedings of the IEEE/CVF international conference on computer vision*, 2019, pp. 4794–4802.
- [22] S. I. Mirzadeh, M. Farajtabar, A. Li, N. Levine, A. Matsukawa, and H. Ghasemzadeh, "Improved knowledge distillation via teacher assistant," in *Proceedings of the AAAI conference on artificial intelligence*, vol. 34, no. 04, 2020, pp. 5191–5198.
- [23] X. Zhou, Y. Tian, and X. Wang, "Mec-da: Memory-efficient collaborative domain adaptation for mobile edge devices," *IEEE Transactions on Mobile Computing*, 2023.
- [24] Y. J. Cho, A. Manoel, G. Joshi, R. Sim, and D. Dimitriadis, "Heterogeneous ensemble knowledge transfer for training large models in federated learning," 2022.
- [25] T. Lin, L. Kong, S. U. Stich, and M. Jaggi, "Ensemble distillation for robust model fusion in federated learning," *Advances in Neural Information Processing Systems*, vol. 33, pp. 2351–2363, 2020.
- [26] J. Hong, H. Wang, Z. Wang, and J. Zhou, "Efficient split-mix federated learning for on-demand and in-situ customization," *arXiv preprint arXiv:2203.09747*, 2022.
- [27] S. Alam, L. Liu, M. Yan, and M. Zhang, "Fedrolex: Model-heterogeneous federated learning with rolling sub-model extraction," 2023.
- [28] E. Diao, J. Ding, and V. Tarokh, "Heterofl: Computation and communication efficient federated learning for heterogeneous clients," 2021.
- [29] E. Shulgin and P. Richtárik, "Towards a better theoretical understanding of independent subnetwork training," *arXiv preprint arXiv:2306.16484*, 2023.
- [30] P. Vepakomma, O. Gupta, T. Swedish, and R. Raskar, "Split learning for health: Distributed deep learning without sharing raw patient data," *arXiv preprint arXiv:1812.00564*, 2018.
- [31] A. Singh, P. Vepakomma, O. Gupta, and R. Raskar, "Detailed comparison of communication efficiency of split learning and federated learning," *arXiv preprint arXiv:1909.09145*, 2019.
- [32] Y. Gao, M. Kim, S. Abuadba, Y. Kim, C. Thapa, K. Kim, S. A. Camtepe, H. Kim, and S. Nepal, "End-to-end evaluation of federated learning and split learning for internet of things," *arXiv preprint arXiv:2003.13376*, 2020.
- [33] C. Thapa, P. C. M. Arachchige, S. Camtepe, and L. Sun, "Splitfed: When federated learning meets split learning," in *Proceedings of the AAAI Conference on Artificial Intelligence*, vol. 36, no. 8, 2022, pp. 8485–8493.
- [34] Y. Chen, Z. Chen, P. Wu, and H. Yu, "Fedodb: Opportunistic block dropout for efficiently training large-scale neural networks through federated learning," *arXiv preprint arXiv:2208.05174*, 2022.
- [35] T. Zhang, T. Feng, S. Alam, M. Zhang, S. S. Narayanan, and S. Avestimehr, "Gpt-fl: Generative pre-trained model-assisted federated learning," *arXiv preprint arXiv:2306.02210*, 2023.
- [36] T. Li, S. Hu, A. Beirami, and V. Smith, "Ditto: Fair and robust federated learning through personalization," in *International conference on machine learning*. PMLR, 2021, pp. 6357–6368.
- [37] A. Fallah, A. Mokhtari, and A. Ozdaglar, "Personalized federated learning: A meta-learning approach," *arXiv preprint arXiv:2002.07948*, 2020.
- [38] L. Collins, H. Hassani, A. Mokhtari, and S. Shakkottai, "Exploiting shared representations for personalized federated learning," in *International conference on machine learning*. PMLR, 2021, pp. 2089–2099.
- [39] A. Beznosikov, S. Horváth, P. Richtárik, and M. Safaryan, "On biased compression for distributed learning," *arXiv preprint arXiv:2002.12410*, 2020.
- [40] M. Safaryan, F. Hanzely, and P. Richtárik, "Smoothness matrices beat smoothness constants: Better communication compression techniques for distributed optimization," *Advances in Neural Information Processing Systems*, vol. 34, pp. 25 688–25 702, 2021.
- [41] B. Wang, M. Safaryan, and P. Richtárik, "Theoretically better and numerically faster distributed optimization with smoothness-aware quantization techniques," *Advances in Neural Information Processing Systems*, vol. 35, pp. 9841–9852, 2022.
- [42] T. Chen, S. Kornblith, M. Norouzi, and G. Hinton, "A simple framework for contrastive learning of visual representations," in *International conference on machine learning*. PMLR, 2020, pp. 1597–1607.
- [43] K. He, H. Fan, Y. Wu, S. Xie, and R. Girshick, "Momentum contrast for unsupervised visual representation learning," in *Proceedings of the IEEE/CVF conference on computer vision and pattern recognition*, 2020, pp. 9729–9738.
- [44] P. Khosla, P. Teterwak, C. Wang, A. Sarna, Y. Tian, P. Isola, A. Maschinot, C. Liu, and D. Krishnan, "Supervised contrastive learning," *Advances in neural information processing systems*, vol. 33, pp. 18 661–18 673, 2020.
- [45] Q. Li, B. He, and D. Song, "Model-contrastive federated learning," in *Proceedings of the IEEE/CVF conference on computer vision and pattern recognition*, 2021, pp. 10 713–10 722.
- [46] Q. Yu, Y. Liu, Y. Wang, K. Xu, and J. Liu, "Multimodal federated learning via contrastive representation ensemble," *arXiv preprint arXiv:2302.08888*, 2023.
- [47] F. Wang and H. Liu, "Understanding the behaviour of contrastive loss," in *Proceedings of the IEEE/CVF conference on computer vision and pattern recognition*, 2021, pp. 2495–2504.
- [48] A. Krizhevsky, G. Hinton *et al.*, "Learning multiple layers of features from tiny images," 2009.
- [49] Y. Le and X. Yang, "Tiny imagenet visual recognition challenge," *CS 231N*, vol. 7, no. 7, p. 3, 2015.
- [50] M. Kim, S. Yu, S. Kim, and S.-M. Moon, "Depthfl: Depthwise federated learning for heterogeneous clients," in *The Eleventh International Conference on Learning Representations*, 2022.
- [51] M. P. Marcus, B. Santorini, and M. A. Marcinkiewicz, "Building a large annotated corpus of English: The Penn Treebank," *Computational Linguistics*, vol. 19, no. 2, pp. 313–330, 1993. [Online]. Available: <https://aclanthology.org/J93-2004>
- [52] D. Yao, W. Pan, M. J. O'Neill, Y. Dai, Y. Wan, H. Jin, and L. Sun, "Fedhm: Efficient federated learning for heterogeneous models via low-rank factorization," 2022.
- [53] K. Bonawitz, V. Ivanov, B. Kreuter, A. Marcedone, H. B. McMahan, S. Patel, D. Ramage, A. Segal, and K. Seth, "Practical secure aggregation for privacy-preserving machine learning," in *proceedings of the 2017 ACM SIGSAC Conference on Computer and Communications Security*, 2017, pp. 1175–1191.
- [54] J. So, C. He, C.-S. Yang, S. Li, Q. Yu, R. E. Ali, B. Guler, and S. Avestimehr, "Lightsecagg: a lightweight and versatile design for secure aggregation in federated learning," *Proceedings of Machine Learning and Systems*, vol. 4, pp. 694–720, 2022.